Phytochemistry Letters 22 (2017) 255–260

Contents lists available at ScienceDirect

Phytochemistry Letters

journal homepage: www.elsevier.com/locate/phytol

Investigation of chemical constituents from *Spiraea prunifolia* var. *simpliciflora* and their biological activities

Chung Sub Kim[a,b], Joonseok Oh[a,b], Won Se Suh[c], Sung Wan Jang[c], Lalita Subedi[d,e], Sun Yeou Kim[d,e], Sang Un Choi[f], Kang Ro Lee[c,*]

[a] *Department of Chemistry, Yale University, New Haven, CT 06520, United States*
[b] *Chemical Biology Institute, Yale University, West Haven, CT 06516, United States*
[c] *Natural Products Laboratory, School of Pharmacy, Sungkyunkwan University, Suwon 16419, Republic of Korea*
[d] *Gachon Institute of Pharmaceutical Science, Gachon University, Incheon 21936, Republic of Korea*
[e] *College of Pharmacy, Gachon University, #191, Hambakmoero, Yeonsu-gu, Incheon 21936, Republic of Korea*
[f] *Korea Research Institute of Chemical Technology, Daejeon 34114, Republic of Korea*

ARTICLE INFO

Keywords:
Spiraea prunifolia var. *simpliciflora*
Phenolic glycosides
GIAO NMR chemical shift calculations
Cytotoxicity
Anti-inflammation
Neuroprotection

ABSTRACT

Quantum mechanics (QM)-based calculations for elucidating full structures of natural compounds are growing in importance and reliability. Two new phenolic glycosides (**1** and **2**) and 11 known compounds were isolated from the twigs of *Spiraea prunifolia* var. *simpliciflora*. The chemical structures of the new compounds (**1** and **2**) were initially established through different NMR techniques (^{1}H and ^{13}C NMR, COSY, HSQC, and HMBC), HRMS data analysis, and chemical hydrolysis. These structure assignments were further verified by QM-based NMR chemical shift calculations. All of the purified compounds (**1–13**) were evaluated for their cytotoxicity against four human cancer cell lines (A549, SK-OV-3, SK-MEL-2, and BT549). Those phytochemicals were also evaluated for both anti-inflammatory activity through the measurement of nitric oxide (NO) production levels in lipopolysaccharide (LPS)-stimulated murine microglia BV-2 cell lines and neuroprotective effects via induction of nerve growth factor (NGF) in C6 glioma cells.

1. Introduction

Spiraea prunifolia var. *simpliciflora* Nakai (Rosaceae), commonly called “bridal wreath,” is a deciduous shrub widely distributed in Korea. The roots of this plant have been used as Korean traditional medicine to treat malaria, fever, and emetic conditions, and its young leaves have been consumed as a salad (Oh et al., 2001). Previous investigation reported that the extracts of *S. prunifolia* var. *simpliciflora* show anti-inflammatory and antipyretic activities (So et al., 1999), and possess terpenoids, flavonoids, and phenolic compounds (Oh et al., 2001; Park et al., 2013; Yean et al., 2014; Youn and Chung, 1987). On the contrary to numerous studies on the roots, there have only been a few investigations of bioactive phytochemicals of the twigs.

Quantum mechanics (QM)-based predictions, for the identification and/or verification of full structures of natural product-originating compounds, are growing in significance and reliability (Lodewyk et al., 2011). These approaches are of particular use in verifying structural assignments, considering erroneous assignment due to a high degree of molecular complexity, human errors, and NMR correlation ambiguities (Grimblat et al., 2015). Despite the utility of synthesis and X-ray crystallography in structural validation and corrections (Nicolaou et al., 2000), such methods can be impractical in terms of costs and unfavorable molecular properties. Alternatively, QM-based calculations of NMR properties, using gauge-including atomic orbitals (GIAO) NMR chemical shift calculations, have been spotlighted as effective protocols for the verification of chemical structure assignments made based upon conventional methods (Grimblat et al., 2015; Kim et al., 2017a; Lodewyk et al., 2011).

In a continuing search for bioactive scaffolds from Korean medicinal plants, we recently reported cytotoxic phenolic compounds from *S. prunifolia* var. *simpliciflora* (Jang et al., 2015). In this study, we isolated and identified two new phenolic compounds, *trans*- and *cis*-pruspirides (**1** and **2**), along with 11 known compounds from this plant (Fig. 1). The chemical structures of purified compounds were determined by 1D and 2D NMR (^{1}H and ^{13}C NMR, COSY, HSQC, and HMBC), HRMS, and LC/MS data analysis. Notably, the initial structural assignment of compound **1** was verified utilizing GIAO-based NMR chemical shift calculations. These phytochemicals (**1–13**) were also assessed for their cytotoxic, anti-inflammatory, and neuroprotective activities employing relevant bioassay approaches.

* Corresponding author.
E-mail address: krlee@skku.edu (K.R. Lee).

http://dx.doi.org/10.1016/j.phytol.2017.09.014
Received 3 July 2017; Received in revised form 11 September 2017; Accepted 22 September 2017

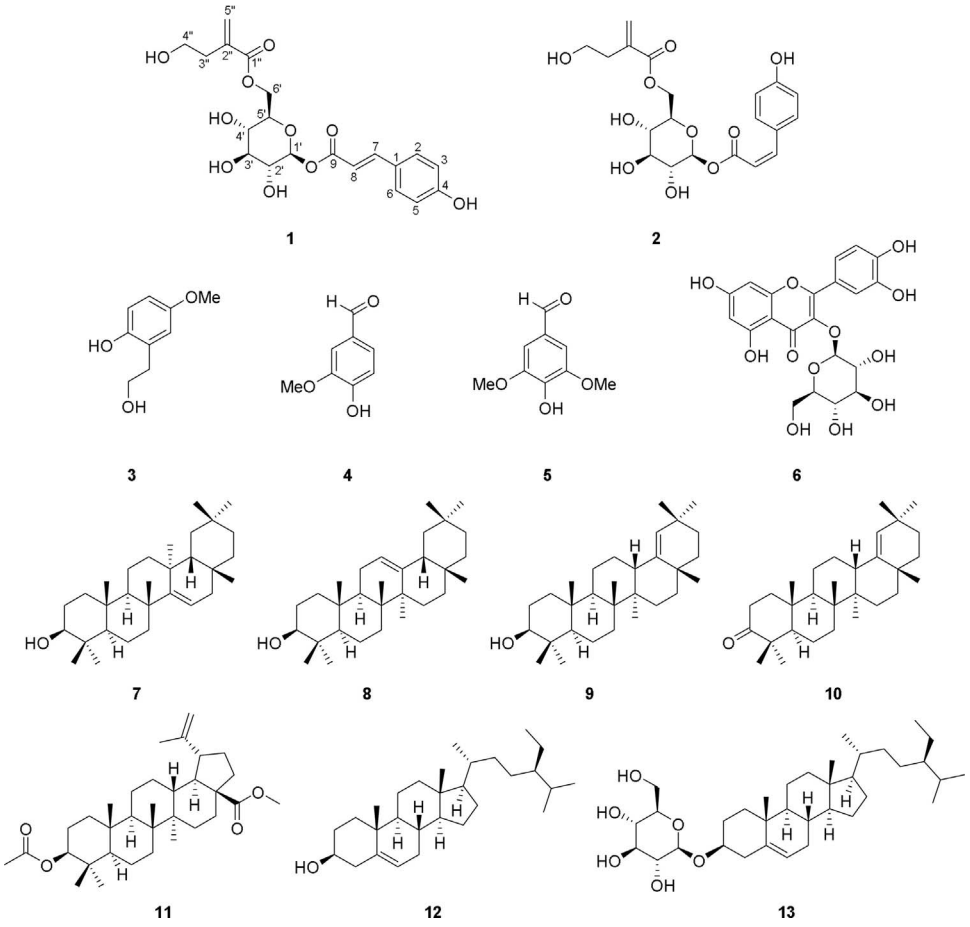

Fig. 1. Chemical structures of compounds **1–13**.

2. Results and discussion

Compound **1** was purified as a colorless gum and its molecular formula was confirmed as $C_{20}H_{24}O_{10}$ based on the protonated HRFABMS molecular ion $[M + H]^+$ at *m/z* 425.1450 (calcd for $C_{20}H_{25}O_{10,}$ 425.1448). The ^{1}H NMR spectrum of **1** exhibited the presence of a *trans*-coumaroyl group [(δ_H 7.76 (1H, d, J = 15.9 Hz), 7.51 (2H, d, J = 8.7 Hz), 6.84 (2H, d, J = 8.7 Hz), and 6.40 (1H, d, J = 15.9 Hz)], a glucopyranosyl moiety [δ_H 5.50 (1H, d, J = 8.1 Hz), 4.51 (1H, dd, J = 12.1, 2.1 Hz), 4.31 (1H, dd, J = 12.1, 5.7 Hz), 3.69 (1H, ddd, J = 9.7, 5.7, 2.1), 3.50 (1H, t, J = 9.0 Hz), 3.46 (1H, dd, J = 9.1, 8.1 Hz), and 3.43 (1H, dd, J = 9.7, 9.0 Hz)], two olefinic protons [δ_H 6.27 (1H, d, J = 1.5 Hz) and 5.72 (1H, dd, J = 1.5, 1.1 Hz)], and two methylenes [δ_H 3.69 (2H, t, J = 6.6 Hz), 2.56 (2H, td, J = 6.6, 1.1 Hz)]. The ^{13}C NMR spectrum of **1** showed 20 resonances characteristic for an ester-like carbonyl (δ_C 168.4), an 1,4-disubstituted aromatic ring [δ_C 161.8, 131.5 (×2), 127.1 (×2), and 117.0], two double bonds (δ_C 148.1, 138.8, 127.7, and 114.6), a glucopyranosyl group (δ_C 95.9, 78.2, 76.5, 74.2, 71.3, and 64.9), an oxygenated carbon (δ_C 61.7), and a methylene carbon (δ_C 36.4). These spectroscopic data (Table 1) were similar to those of 1-caffeoyl-6-tuliposide A (Park et al., 2013), except for the presence of resonances for an 1,4-disubstituted aromatic ring in **1** (see above) instead of those for an 1,2,4-trisubstituted aromatic ring [δ_C 148.2, 145.4, 126.3, 121.5, 115.1, and 113.8; δ_H 7.06 (1H, d, J = 1.8 Hz), 6.97 (1H, dd, J = 8.4, 1.8 Hz), and 6.78 (1H, d, J = 8.4 Hz)] in 1-caffeoyl-6-tuliposide A.

The 2D structure of **1** was established by analyses of 2D NMR data including COSY, HSQC, and HMBC, and the connectivities among the *trans*-coumaroyl group, glucopyranose, and 4-hydroxy-2-methylenebutanoyl moiety were established via the HMBC cross peaks of H-1′/C-9 and H-6′/C-1″ (Fig. 2). The monosaccharide unit was assumed to be β-glucopyranose by the associated chemical shifts of the ^{1}H and ^{13}C resonances, which was confirmed by the relatively large coupling constants between H-1′/H-2′ (8.1 Hz), H-2′/H-3′ (9.1 Hz), H-3′/H-4′ (9.0 Hz), and H-4′/H-5′ (9.7 Hz). To establish the absolute configuration of the glucopyranosyl motif, compound **1** was hydrolyzed and

Table 1
^{1}H [ppm, mult., (J in Hz)] and ^{13}C NMR spectroscopic data of compounds **1** and **2** in methanol-d_4 and calculated ^{13}C NMR data of **1**.

position	**1**			**2**	
	δ_H	δ_C (exp.)	δ_C (cal.)	δ_H	δ_C
1		127.1	123.4		127.5
2/6	7.51, d (8.7)	131.5	129.1	7.72, d (8.7)	134.4
3/5	6.84, d (8.7)	117.0	111.4	6.77, d (8.7)	116.0
4		161.8	156.8		160.7
7	7.76, d (15.9)	148.1	144.3	6.97, d (12.8)	147.4
8	6.40, d (15.9)	114.6	108.0	5.84, d (12.8)	115.6
9		167.9	165.5		166.6
1′	5.50, d (8.1)	95.9	99.9	5.55, d (8.2)	95.7
2′	3.46, dd (9.1, 8.1)	74.2	77.1	3.39, dd (9.1, 8.2)	74.1
3′	3.50, t (9.0)	78.2	79.9	3.48, t (9.1)	78.3
4′	3.43, dd (9.7, 9.0)	71.3	71.2	3.41, dd (9.7, 9.1)	71.3
5′	3.69, ddd (9.7, 5.7, 2.1)	76.5	76.9	3.67, ddd (9.7, 5.8, 2.1)	76.3
6′a	4.51, dd (12.1, 2.1)	64.9	66.9	4.52, dd (12.0, 2.1)	64.9
6′b	4.31, dd (12.1, 5.7)			4.31, dd (12.0, 5.8)	
1″		168.4	166.0		169.1
2″		138.8	140.4		138.8
3″	2.56, td (6.6, 1.1)	36.4	40.6	2.57, td (6.7, 1.1)	36.5
4″	3.69, t (6.6)	61.7	66.6	3.69, t (6.7)	61.7
5″a	6.27, d (1.5)	127.7	127.7	6.28, d (1.5)	127.7
5″b	5.72, dd (1.5, 1.1)			5.72, dd (1.5, 1.1)	

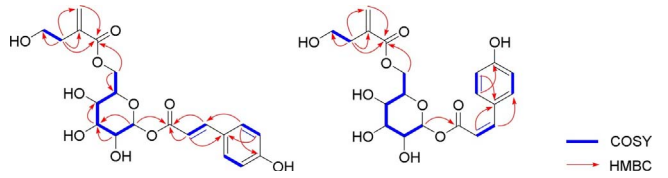

Fig. 2. Key COSY (blue bold) and HMBC (red arrows) correlations of **1** and **2**. (For interpretation of the references to colour in this figure legend, the reader is referred to the web version of this article.)

derivatized with L-cysteine methyl ester hydrochloride and *o*-tolyl isothiocyanate (Tanaka et al., 2007). The LC/MS analysis was performed for the derivative of **1** with those of authentic D- and L-glucopyranose samples. The results revealed that retention time of the glucopyranose derivative from compound **1** was identical to that from the standard D-glucopyranose, confirming the presence of β-D-glucopyranose moiety in **1**. Consequently, the structure of **1** was determined as 1-*O*-*trans*-*p*-coumaroyl-6-*O*-(4-hydroxy-2-methylenebutanoyl)-β-D-glucopyranose. The trivial name *trans*-pruspiride was assigned to **1**.

The structural assignment of compound **1** was further confirmed by the comparison of the experimental and computed ^{13}C NMR chemical shift values (Kim et al., 2017a, 2017b; Lodewyk et al., 2011; Smith and Goodman, 2010; Waters et al., 2015). Major conformers of **1** were identified upon conformational searches utilizing Macromodel (Schrödinger LLC) and further optimized using the B3LYP hybrid density-functional theory (DFT) method with the 6–31 + G(d,p) basis set (Fig. 3). The NMR shielding properties of those conformers were calculated employing GIAO-based NMR chemical shift calculations using the identical basis set for optimization. The computed ^{13}C NMR chemical shift data for **1** (Table 1) were plotted with the experimental data (Fig. 4). The statistical analysis of the experimental and the calculated ^{13}C NMR chemical shift values exhibited an excellent correlation slope with the R^2 value of 0.9954, verifying our initial structural establishment of **1**.

Compound **2** was obtained as a colorless gum with the identical molecular formula to that of **1** ($C_{20}H_{25}O_{10}$, 425.1448), given its HRFABMS data displaying the protonated ion $[M + H]^+$ at *m/z* 425.1445 (calcd for $C_{20}H_{25}O_{10}$, 425.1448). Inspection of the ^{1}H and ^{13}C NMR data of **2** (Table 1) suggested that this compound shared close structural similarities with **1**. The significant difference was the geometry of the *p*-coumaroyl moiety; the coupling constant between H-7 and H-8 in **2** was 12.8 Hz whereas that was 15.9 Hz in **1**, which implied that **2** possessed *cis*-geometry of *p*-coumaroyl moiety. Full NMR analysis

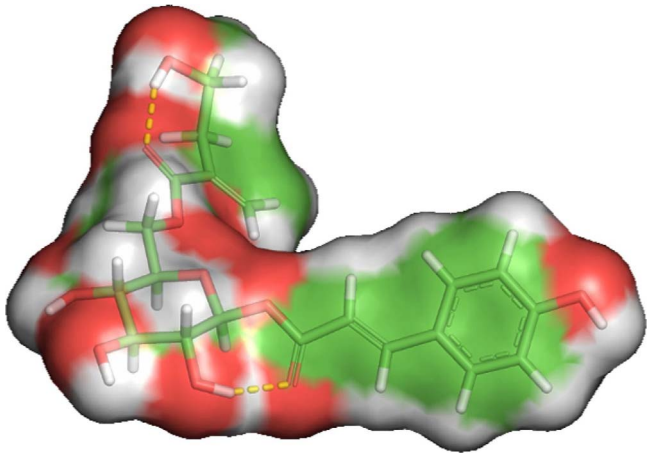

Fig. 3. 3D structure of compound **1** and its surface model minimized at the MMFF force field and subsequently optimized at the B3LYP/6–31 + G(d,p) level. Yellow dashed lines represent hydrogen bonding, and red represents oxygen and green and white represent carbon and hydrogen, respectively. (For interpretation of the references to colour in this figure legend, the reader is referred to the web version of this article.)

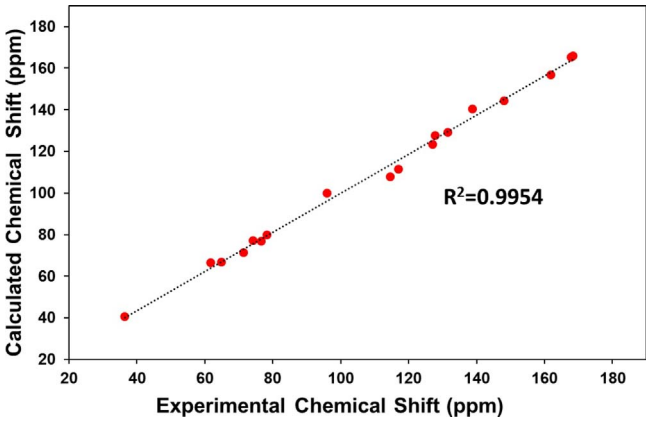

Fig. 4. Statistical analysis of experimental and computed ^{13}C NMR chemical shift values of **1**.

including COSY, HSQC, and HMBC confirmed the chemical structure of **2** (Fig. 2). Thus, the structure of **2** was established as 1-*O*-*cis*-*p*-coumaroyl-6-*O*-(4-hydroxy-2-methylenebutanoyl)-β-D-glucopyranose, and the trivial name *cis*-pruspiride was given to **2**.

Other 11 compounds were identified as 2-(2-hydroxy-5-methoxyphenyl)ethanol (**3**) (Lal et al., 1987), vanillin (**4**) (Kim et al., 2003), syringaldehyde (**5**) (Kim et al., 2003), quercetin 3-*O*-β-D-glucopyranoside (**6**) (Markham et al., 1978), taraxerol (**7**) (Sakurai et al., 1986), β-amyrin (**8**) (Lima et al., 2004), germanicol (**9**) (Kim et al., 2005), germanicone (**10**) (Frontana et al., 1994), methyl 3-*O*-acetylbetulinate (**11**) (Kommera et al., 2010), β-sitosterol (**12**) (Ahmad et al., 2010), and sitosterol-3-*O*-β-D-glucopyranoside (**13**) (Kojima et al., 1990) based on their observed and reported spectroscopic data.

The cytotoxicity of the isolates (**1–13**) was evaluated against four human cancer cell lines, A549, SK-OV-3, SK-MEL-2, and BT549. As shown in Table 2, compounds **8**, **11**, and **12** exhibited weak cytotoxicity possessing IC_{50}'s ranging from 23.59 to 29.71 μM. Among four lupane-type triterpenoids (**7–10**) only compound **8** (β-amyrin) displayed cytotoxicity against SK-OV-3 cell line (IC_{50} 29.71 μM), while the others were inactive (IC_{50} > 30 μM). Interestingly, compound **9** (germanicol), a regioisomer of **8**, with different double bond positioned between C-18 and C-19, was not active, demonstrating that the olefinic bond location at C-12 and C-13 appears to play an important role in exerting cytotoxic activity of lupane-type triterpenoids. Moreover, sitosterol-3-*O*-β-D-glucopyranoside (**13**) displayed no activity whereas its aglycone **12** showed cytotoxicity against A549 cell line (IC_{50} 29.02 μM), implying that such monosaccharide moieties might be involved in nullifying cytotoxicity.

The anti-inflammatory effects on the purified phytochemicals (**1–13**) were tested through the measurement of NO production levels in the LPS-stimulated murine microglia BV-2 cell line (Table 3). Compounds **4** and **11** exerted moderate inhibition of NO production with IC_{50}'s of 88.12 and 93.10 μM without significant cell toxicity

Table 2
Cytotoxicity of selected compounds against four cultured human cancer cell lines in the SRB bioassay.

Comp.	IC_{50} (μM)[a]			
	A549	SK-OV-3	SK-MEL-2	BT549
8	> 30.0	29.71	> 30.0	> 30.0
11	> 30.0	23.59	> 30.0	26.52
12	29.02	> 30.0	> 30.0	> 30.0
Cisplatin[b]	1.69	2.81	1.44	1.62

[a] 50% inhibitory concentration; the concentration of compound that caused a 50% inhibition in cell growth.
[b] Positive control.

Table 3
Inhibitory effect of compounds **1–13** on NO production in LPS-activated BV-2 cells.

Comp.	IC_{50} (μM)[a]	Cell viability (%)[b]	Comp.	IC_{50} (μM)[a]	Cell viability (%)[b]
1	349.21	94.38 ± 12.97	**8**	156.67	88.84 ± 8.79
2	139.39	95.21 ± 11.71	**9**	191.96	79.55 ± 6.49
3	> 500	105.27 ± 15.90	**10**	> 500	79.78 ± 6.69
4	88.12	115.33 ± 6.73	**11**	93.10	82.08 ± 4.42
5	430.89	120.62 ± 8.41	**12**	131.73	92.27 ± 4.13
6	300.55	100.17 ± 11.35	**13**	195.45	87.69 ± 5.23
7	> 500	79.26 ± 5.29	L-NMMA[c]	21.82	114.08 ± 2.96

[a] IC_{50} value of each compound was defined as the concentration (μM) that caused 50% inhibition of NO production in LPS-activated BV-2 cells.
[b] Cell viability following treatment with 20 μM of each compound was determined using the MTT assay and is expressed as a percentage (%). Data are expressed as the mean ± standard deviation (SD) of three independent experiments.
[c] Positive control.

(115.33 ± 6.73 and 82.08 ± 4.42%). Compound **5**, a C-5 methoxylated derivative of **4**, exhibited poor activity (IC_{50} 430.89 μM), which was indicative of the methoxy group at C-5 in benzaldehyde being a diminishing factor in the production of NO in BV-2 cell. The other compounds showed weak or no activity.

The neuroprotective activities of the isolated compounds (**1–13**) were also evaluated by assessing their induction potentials on NGF secretion in C6 cells (Table 4). All tested compounds displayed moderate to weak activities with stimulatory levels ranging from 88.40 ± 8.71 to 138.98 ± 9.49% without substantial cell toxicity at the tested concentration (20 μM). Among the compounds **1–13**, the two new compounds (**1** and **2**), and **11** were relatively potent stimulants of NGF release (138.98 ± 9.49, 123.38 ± 6.16, and 126.80 ± 6.73%, respectively).

3. Experimental

3.1. General experimental procedures

Optical rotation data were recorded utilizing a JASCO P-1020 polarimeter (JASCO, Easton, MD, USA). Ultraviolet (UV) spectra were garnered using a Shimadzu UV-1601 UV–vis spectrophotometer (Shimadzu, Tokyo, Japan). The NMR studies were accomplished employing a Bruker AVANCE III 700 NMR spectrometer and resultant spectra were processed using MestReNova (Mnova) 10.0 with default weighting functions. HRFABMS data were acquired on a Waters SYNAPT G2 (Milford, MA, USA). The HPLC-DAD-MS data were measured using an Agilent 1260 Infinity HPLC system (Agilent, Santa Clara, CA, USA) using a Kinetex C_{18} 5 μm column (250 mm length × 4.6 mm i.d.; Phenomenex, Torrance, CA, USA). Purification was achieved using a semi-preparative HPLC system equipped with a Gilson 306 pump (Middleton, WI, USA), a Shodex refractive index detector (New York, NY, USA), and a Luna C_{18} 10 μm column (250 mm length × 10 mm i.d.; Phenomenex, Torrance, CA, USA) or an Apollo Silica 5 μm column (250 mm length × 10 mm i.d.; Apollo, Manchester, UK). Open columns packed with silica gel 60 (70–230 and 230–400 mesh; Merck) or RP-C_{18} silica gel (230–400 mesh; Merck, Darmstadt, Germany) were implemented for crude fractionation and separation. Precoated silica gel F_{254} plates and RP–18 F_{254s} plates (Merck) were utilized for thin-layer chromatography (TLC).

3.2. Plant material

The twigs of *S. prunifolia* var. *simpliciflora* were collected from Goesan, Republic of Korea in March 2013, and the plant material was authenticated by one of the authors (K. R. L.). A voucher specimen, coded SKKU-NPL 1301, was deposited in the herbarium of the School of Pharmacy, Sungkyunkwan University, Suwon, Republic of Korea.

3.3. Extraction and isolation

The dried twigs of *S. prunifolia* var. *simpliciflora* (7 kg) were extracted with 80% aqueous MeOH under reflux and crude extract was filtered. The filtrate was evaporated to acquire the crude extract (380 g). The crude was suspended in H_2O, and partitioned with *n*-hexane, $CHCl_3$, EtOAc, and *n*-butanol, yielding 28, 29, 12, and 47 g of the respective residues. The *n*-hexane-soluble fraction (15 g) was subjected to a normal phase open column chromatography (*n*-hexane:EtOAc, 10:1 → 1:1) to generate seven fractions (H1–H7). Fraction H1 (1.2 g) was chromatographed on a silica gel open column (*n*-hexane:EtOAc, 40:1) and further purified by semi-preparative silica gel HPLC (2 mL/min; *n*-hexane:EtOAc, 25:1) to obtain **11** (20 mg). Compound **10** (12 mg) was furnished upon the purification of fraction H2 (2.3 g) with a silica gel open column (*n*-hexane:EtOAc, 40:1) followed by semi-preparative silica gel HPLC (2 mL/min; *n*-hexane:EtOAc, 25:1). Fraction H3 (1.4 g) was applied to a normal phase open column chromatography (silica; *n*-hexane:EtOAc, 40:1) and further purified using semi-preparative silica gel HPLC (2 mL/min; *n*-hexane:EtOAc,

Table 4
Effects of compounds **1-13** on NGF secretion in C6 cells.

Comp.	NGF secretion (%)[a]	Cell viability (%)[b]	Comp.	NGF secretion (%)[a]	Cell viability (%)[b]
1	138.98 ± 9.49	82.14 ± 0.44	**8**	96.39 ± 7.56	94.86 ± 3.27
2	123.38 ± 6.16	78.06 ± 0.47	**9**	104.18 ± 4.17	101.14 ± 2.29
3	104.18 ± 12.59	98.49 ± 8.27	**10**	88.40 ± 8.71	96.00 ± 0.78
4	119.90 ± 6.84	116.58 ± 2.73	**11**	126.80 ± 6.73	106.80 ± 0.35
5	111.47 ± 13.67	104.03 ± 3.59	**12**	103.74 ± 7.36	93.02 ± 0.757
6	100.22 ± 7.43	111.85 ± 5.28	**13**	111.07 ± 13.26	96.55 ± 0.14
7	95.63 ± 6.69	61.50 ± 0.35	6-Shogaol[c]	168.58 ± 7.16	125.80 ± 0.93

[a] C6 cells were treated with 20 μM of each compound. After 24 h, the content of NGF secreted in the C6-conditioned medium was measured by ELISA. The level of secreted NGF is expressed as the percentage of the untreated control (set as 100%).
[b] Cell viability after treatment with 20 μM of each compound was determined by an MTT assay and is expressed as a percentage (%). Results are the means of three independent experiments, and the data are expressed as mean ± SD.
[c] Positive control.

25:1) to give **12** (60 mg). Compound **7** (24 mg) was obtained by separation of fraction H4 (1.5 g) with a silica gel open column ($CHCl_3$:MeOH, 40:1) followed by the recrystallization in MeOH.

The $CHCl_3$-soluble fraction (19 g) was subjected to a normal phase open column chromatography ($CHCl_3$:MeOH, 30:1 → 1:1) to yield 10 fractions (C1–C10). Fraction C1 (1.0 g) was fractionated utilizing a normal phase open column chromatography (*n*-hexane:EtOAc:MeOH, 15:1:0.5) and further purified using semi-preparative silica gel or RP-C_{18} silica gel HPLC (2 mL/min; *n*-hexane:EtOAc, 25:1 or 40% aqueous MeOH) to give **4** (5 mg), **5** (7 mg), **8** (21 mg), and **9** (14 mg). Compound **3** (6 mg) was obtained from fraction C3 (0.6 g) employing an RP-C_{18} silica gel open column with a programmed gradient (40% → 100% aqueous MeOH) and semi-preparative silica gel HPLC (2 mL/min; *n*-hexane:EtOAc:MeOH, 5:1:1). Fraction C5 (3.4 g) was applied to an RP-C_{18} silica gel open column (50% → 100% aqueous MeOH) and further purified by semi-preparative silica gel HPLC (2 mL/min; *n*-hexane:EtOAc:MeOH, 10:1:1) to acquire **13** (16 mg).

The EtOAc-soluble fraction (10 g) was subjected to a normal phase open column chromatography ($CHCl_3$:MeOH:H_2O, 4:1:0.1) to yield seven fractions (E1–E7). The fraction E3 (0.8 g) was isolated using an RP-C_{18} silica gel open column (40% → 100% aqueous MeOH) and successively semi-preparative RP-C_{18} silica gel HPLC (2 mL/min; 20% aqueous MeCN) was applied to obtain **1** (9 mg) and **2** (4 mg). Compound **6** (7 mg) was furnished upon the purification of fraction E4 (1.4 g) with an RP-C_{18} silica gel open column (40% → 100% aqueous MeOH) followed by the semi-preparative RP-C_{18} silica gel HPLC (2 mL/min; 20% aqueous MeCN).

3.3.1. *trans-pruspiride (**1**)*

Colorless gum; [α] + 10 (*c* 0.1, MeOH); IR (KBr) ν_{max} cm^{-1}: 3388, 2940, 1690, 1599, 1156, 1083; UV (MeOH) λ_{max} (log ε) 309 (3.45), 234 (3.30) nm; ^1H (700 MHz) and ^{13}C NMR (175 MHz) data, see Table 1; HRFABMS (positive-ion mode) *m/z* 425.1450 $[M + H]^+$ (calcd for $C_{20}H_{25}O_{10,}$ 425.1448).

3.3.2. *cis-pruspiride (**2**)*

Colorless gum; [α] + 15 (*c* 0.1, MeOH); IR (KBr) ν_{max} cm^{-1}: 3389, 2941, 1688, 1601, 1157, 1082; UV (MeOH) λ_{max} (log ε) 290 (3.32), 231 (3.29) nm; ^1H (700 MHz) and ^{13}C NMR (175 MHz) data, see Table 1; HRFABMS (positive-ion mode) *m/z* 425.1445 $[M + H]^+$ (calcd for $C_{20}H_{25}O_{10,}$ 425.1448).

3.4. *Acid hydrolysis of **1** and **2** and sugar analysis*

Compounds **1** and **2** (1 mg) were individually hydrolyzed with 1 N HCl (1 mL) under reflux for 2 h. $CHCl_3$ was used to extract organic layers from each reaction mixture. The monosaccharide residues were acquired from each reaction mixture of the H_2O-soluble phases upon neutralization using an Amberlite IRA-67 resin. The monosaccharides were added to pyridine (0.5 mL) containing L-cysteine methyl ester hydrochloride (0.5 mg) and the respective reaction mixtures were stirred at 60 °C for 1 h. Then *o*-tolyl isothiocyanate (0.1 mL) was added and stirred at 60 °C for another 1 h. Each reaction mixture was analyzed without purification by LC/MS analysis (0.7 mL/min; 25% aqueous MeCN with 0.1% formic acid for 30 min). The hydrolysate derivatives of **1** and **2** were detected at 13.6 min and the authentic D- and L-glucopyranose samples were at 13.6 min and 12.6 min, respectively, verifying that the glycosidic moieties from the two compounds were both D-configured.

3.5. *GIAO-based NMR chemical shift calculations of **1** (Lodewyk et al., 2011; Smith and Goodman, 2010; Waters et al., 2015)*

GIAO-based chemical shift predictions were performed with reference to our previous communication (Kim et al., 2017a). Conformational searches were carried out using MacroModel in the MMFF force field (gas phase), a 10 kcal/mol upper energy limit, and 0.001 kJ $(mol\ Å)^{-1}$ convergence threshold on the rms gradient. The geometries of all the conformers of **1** were optimized utilizing the B3LYP/6–31 + G(d,p) level in the gas phase. The GIAO magnetic shielding tensors of those identified conformers were calculated at the B3LYP/6–31 + G(d,p) level in the polarizable continuum model (PCM) mode with a dielectric constant representing methanol and averaged based on the Boltzmann populations of each conformer in the associated Gibbs free energy. The chemical shift values were calculated via the following equation: $\delta^x_{calcd} = (\sigma^0 - \sigma^x)/(1 - \sigma^0/10^6)$, where δ^x_{calcd} is the calculated NMR chemical shift for nucleus *x*, σ^x and σ^0 are the respective calculated isotropic constants for nucleus *x* and tetramethylsilane (TMS) calculated at the above-mentioned basis sets.

3.6. *Cytotoxicity assessment*

The cytotoxicity of purified metabolites were tested against the A549 (non-small cell lung adenocarcinoma), SK-OV-3 (ovary malignant ascites), SK-MEL-2 (skin melanoma), and BT549 (invasive ductal carcinoma), utilizing the sulforhodamine B colorimetric (SRB) method. Cisplatin (≥98%; Sigma-Aldrich) served as a positive control.

3.7. *Assessment of NO generation and cell viability*

The BV-2 cells, developed by Dr. V. Bocchini at the University of Perugia (Perugia, Italy), were used for this study (Blasi et al., 1990; Choi et al., 2009). The cells were seeded in a 96-well plate (4×10^4 cells/well) and incubated in the presence or absence of various doses of tested compounds. Lipopolysaccharide (LPS) (100 ng/mL) was added to BV-2 cells and grown for 1 d. The produced levels of nitrite (NO_2), a soluble oxidized product of NO, was evaluated with 0.1% *N*-1-napthylethylenediamine dihydrochloride and 1% sulfanilamide in 5% phosphoric acid, aka the Gries reagent. The supernatant (50 μL) was mixed with the Gries reagent (50 μL). After 10 min the absorbance was gauged at 570 nm. For a positive control, the reported nitric oxide synthase (NOS) inhibitor L-NMMA was employed. Graded sodium nitrite solution was utilized to determine nitrite concentrations. An MTT assay was used for the cell viability assay.

3.8. *Nerve growth factor (NGF) and cell viability assays*

The C6 cells (Korean Cell Line Bank, Seoul, Republic of Korea) were seeded in a 24-well plate at (1×10^5 cells/well). After 1 d, the cells were applied with serum-free DMEM together with various doses of the phytochemicals for another day. From the cultured plates, the medium supernatant was collected and the changes in NGF release were measured utilizing an ELISA kit. The viability of the C6 cells was evaluated via an MTT assay. The outcomes were shown as a percentage compared to the negative control (i.e., untreated cells). The positive control was 6-shogaol.

4. Conclusions

In summary, our current study describes the isolation and characterization of 13 chemical constituents, including two new compounds (**1** and **2**), from the twigs of *S. prunifolia* var. *simpliciflora*. The structures of two new secondary metabolites (**1** and **2**) were determined via full analysis of NMR (^1H and ^{13}C NMR, COSY, HSQC, and HMBC) and HRMS, chemical methods, and NMR chemical shift calculations. In particular, the current study shows how GIAO-based NMR calculations can be of great use in validating NMR-based structural assignments.

The identified molecules (**1–13**) were assessed for their cytotoxic, anti-inflammatory, and neuroprotective activities utilizing relevant bioassay protocols. Among them, compounds **8**, **11**, and **12** showed moderate cytotoxic properties against some of four tested human cancer cell lines, compounds **4** and **11** demonstrated mild inhibition of NO

production in the LPS-stimulated murine microglia BV-2 cell line, and compounds **1**, **2**, and **11** were weak stimulants of NGF secretion in C6 cells. These results may constitute a basis for follow-up studies with emphasis on medicinal chemical or phytochemical investigations.

Acknowledgements

This work was supported by the Postdoctoral Research Program of Sungkyunkwan University (2016). We are also thankful to the Korea Basic Science Institute (KBSI) for the measurements of mass spectra.

Appendix A. Supplementary data

Supplementary data associated with this article can be found, in the online version, at https://doi.org/10.1016/j.phytol.2017.09.014.

References

Ahmad, F., Ali, M., Alam, P., 2010. New phytoconstituents from the stem bark of *Tinospora cordifolia* Miers. Nat. Prod. Res. 24, 926–934.

Blasi, E., Barluzzi, R., Bocchini, V., Mazzolla, R., Bistoni, F., 1990. Immortalization of murine microglial cells by a v-raf/v-myc carrying retrovirus. J. Neuroimmunol. 27, 229–237.

Choi, Y., Lee, M.K., Lim, S.Y., Sung, S.H., Kim, Y.C., 2009. Inhibition of inducible NO synthase, cyclooxygenase-2 and interleukin-1β by torilin is mediated by mitogen-activated protein kinases in microglial BV2 cells. Br. J. Pharmacol. 156, 933–940.

Frontana, B., Cárdenas, J., Rodríguez-Hahn, L., 1994. Diterpenoids from *Salvia coulteri*. Phytochemistry 36, 739–741.

Grimblat, N., Zanardi, M.M., Sarotti, A.M., 2015. Beyond DP4: an improved probability for the stereochemical assignment of isomeric compounds using quantum chemical calculations of NMR shifts. J. Org. Chem. 80, 12526–12534.

Jang, S.W., Suh, W.S., Kim, C.S., Kim, K.H., Lee, K.R., 2015. A new phenolic glycoside from *Spiraea prunifolia* var. *simpliciflora* twigs. Arch. Pharm. Res. 38, 1943–1951.

Kim, H., Ralph, J., Lu, F., Ralph, S.A., Boudet, A.-M., MacKay, J.J., Sederoff, R.R., Ito, T., Kawai, S., Ohashi, H., 2003. NMR analysis of lignins in CAD-deficient plants: part 1. Incorporation of hydroxycinnamaldehydes and hydroxybenzaldehydes into lignins. Org. Biomol. Chem. 1, 268–281.

Kim, D.K., Lim, J.P., Kim, J.W., Park, H.W., Eun, J.S., 2005. Antitumor and antiinflammatory constituents from *Celtis sinensis*. Arch. Pharm. Res. 28, 39–43.

Kim, C.S., Oh, J., Subedi, L., Kim, S.Y., Choi, S.U., Lee, K.R., 2017a. Holophyllane A: a triterpenoid possessing an unprecedented B-nor-3, 4-seco-17, 14-friedo-lanostane architecture from *Abies holophylla*. Sci. Rep. 7, 43646.

Kim, C.S., Subedi, L., Oh, J., Kim, S.Y., Choi, S.U., Lee, K.R., 2017b. Bioactive triterpenoids from the twigs of *Chaenomeles sinensis*. J. Nat. Prod. 80, 1134–1140.

Kojima, H., Sato, N., Hatano, A., Ogura, H., 1990. Sterol glucosides from *Prunella vulgaris*. Phytochemistry 29, 2351–2355.

Kommera, H., Kaluđerović, G.N., Kalbitz, J., Paschke, R., 2010. Synthesis and anticancer activity of novel betulinic acid and betulin derivatives. Arch. Pharm. 343, 449–457.

Lal, K., Ghosh, S., Salomon, R.G., 1987. Hydroxyl-directed regioselective monodemethylation of polymethoxyarenes. J. Org. Chem. 52, 1072–1078.

Lima, M., Braga, P.A., Macedo, M.L., Silva, M., Ferreira, A.G., Fernandes, J.B., Vieira, P.C., 2004. Phytochemistry of *Trattinnickia burserifolia*, *T. rhoifolia*, and *Dacryodes hopkinsii*: chemosystematic implications. J. Braz. Chem. Soc. 15, 385–394.

Lodewyk, M.W., Siebert, M.R., Tantillo, D.J., 2011. Computational prediction of 1H and 13C chemical shifts A useful tool for natural product, mechanistic, and synthetic organic chemistry. Chem. Rev. 112, 1839–1862.

Markham, K., Ternai, B., Stanley, R., Geiger, H., Mabry, T., 1978. Carbon-13 NMR studies of flavonoids—III: Naturally occurring flavonoid glycosides and their acylated derivatives. Tetrahedron 34, 1389–1397.

Nicolaou, K., Vourloumis, D., Winssinger, N., Baran, P.S., 2000. The art and science of total synthesis at the dawn of the twenty-first century. Angew. Chem. Int. Ed. 39, 44–122.

Oh, H., Oh, G.-S., Seo, W.-G., Pae, H.-O., Chai, K.-Y., Kwon, T.-O., Lee, Y.-H., Chung, H.-T., Lee, H.-S., 2001. Prunioside A: A new terpene glycoside from *Spiraea prunifolia*. J. Nat. Prod. 64, 942–944.

Park, S.H., Park, K.H., Oh, M.H., Kim, H.H., Choe, K.I., Kim, S.R., Park, K.J., Lee, M.W., 2013. Anti-oxidative and anti-inflammatory activities of caffeoyl hemiterpene glycosides from *Spiraea prunifolia*. Phytochemistry 96, 430–436.

Sakurai, N., Yaguchi, Y., Inoue, T., 1986. Triterpenoids from *Myrica rubra*. Phytochemistry 26, 217–219.

Smith, S.G., Goodman, J.M., 2010. Assigning stereochemistry to single diastereoisomers by GIAO NMR calculation: the DP4 probability. J. Am. Chem. Soc. 132, 12946–12959.

So, H.-S., Park, R., Oh, H.-M., Pae, H.-O., Lee, J.-H., Chai, K.-Y., Chung, S.-Y., Chung, H.-T., 1999. The methanol extract of Spiraea prunifolia var. simpliciflora root inhibits the generation of nitric oxide and superoxide in RAW 264. 7 cells. J. Ethnopharmacol. 68, 209–217.

Tanaka, T., Nakashima, T., Ueda, T., Tomii, K., Kouno, I., 2007. Facile discrimination of aldose enantiomers by reversed-phase HPLC. Chem. Pharm. Bull. 55, 899–901.

Waters, A.L., Oh, J., Place, A.R., Hamann, M.T., 2015. Stereochemical studies of the karlotoxin class using NMR spectroscopy and DP4 chemical-shift analysis: insights into their mechanism of action. Angew. Chem. Int. Ed. 54, 15705–15710.

Yean, M.H., Kim, J.S., Kang, S.S., Kim, Y.S., 2014. A new megastigmane glucoside and three new flavonoid glycosides from *Spiraea prunifolia* var. simpliciflora. Helv. Chim. Acta 97, 1123–1131.

Youn, H.-S., Chung, B.-S., 1987. Studies on the Constituents of the Roots of *Spiraea prunifolia* var *simpliciflora*. Kor. J. Pharmacogn. 18, 107–111.